Received Date : 16-Sep-2018

Revised Date : 05-Nov-2018

Accepted Date : 13-Nov-2018

Cooperativity in proton sensing by PIP aquaporins

Victoria Vitali[1,2†], Cintia Jozefkowicz[3,4†], Agustina Canessa Fortuna[1,2], Gabriela Soto[3,4], F. Luis Gonzalez Flecha[1‡], Karina Alleva[1,2‡].

[1]Universidad de Buenos Aires, CONICET, Instituto de Química y Fisicoquímica Biológica (IQUIFIB), Facultad de Farmacia y Bioquímica, Buenos Aires, Argentina, [2] Universidad de Buenos Aires, Facultad de Farmacia y Bioquímica, Departamento de Fisicomatemática, Buenos Aires, Argentina, [3]Instituto Nacional de Tecnología Agropecuaria, INTA, Castelar, Argentina, [4]CONICET, Buenos Aires, Argentina.

[†]These authors contributed equally.
[‡]These authors contributed equally.

For correspondence:
F. Luis González Flecha (lgf@qb.ffyb.uba.ar) & Karina Alleva (+54 1152874552, kalleva@ffyb.uba.ar)

Running title: PIP aquaporin cooperativity

Article type : Original Article

Abbreviations: AQP, aquaporin; PIP, plasma membrane intrinsic protein; $P_{f,}$ osmotic water permeability coefficient

Keywords: aquaporin, cooperativity, stoichiometry, paralogues, water transport

ABSTRACT

One of the most intriguing properties of PIP aquaporins is their ability to modulate water transport by sensing different levels of intracellular pH through the assembly of homo- and heterotetrameric molecular species in the plasma membrane. In this work, using a phenomenological modeling approach, we demonstrate that cooperativity in PIP biological response cannot be directly attributed to a cooperative proton binding, as it is usually considered, since it could also be the consequence of a cooperative conformation transition between open and closed states of the channel. Moreover, our results show that, when mixed populations of homo- and heterotetrameric PIP channels are co-expressed in the plasma membrane of the same cell, the observed decrease in the degree of positive cooperativity would result from the simultaneous presence of molecular species with different levels of proton sensing. Indeed, the random mixing between different PIP paralogues as subunits in a single tetramer, plus the possibility of mixed populations of homo- and heterotetrameric PIP channels widen the spectrum of cooperative responses of a cell membrane. Our approach offers a deep understanding of cooperative transport of aquaporin channels, as members of a multiprotein family where the relevant proton binding sites of each member have not been clearly elucidated yet.

INTRODUCTION

Cooperative regulation of protein function is a phenomenon of central importance in many cellular processes. This kind of regulatory process is denoted as those biological responses that follow a sigmoidal pattern, instead of hyperbolic, when ligand concentration is increased. Commonly, this sigmoidal behavior has been interpreted as the consequence of changes in affinity for ligands as the reaction progress, i.e. the affinity of a given binding site for a ligand will be affected by the occupancy of other sites by the same or other ligands. However, the biological activity often goes beyond ligand binding since the progress of the reaction (in case of enzymes) or transport events (in case of channels) usually involves conformational changes that optimize the active site or the pore structure. In this regard, two separated events (at least) can be recognized in a cooperative response in most proteins: ligand binding and conformational information transduction. These two steps have been recognized in mechanistic models proposed to explain cooperative phenomena, such as the concerted model [1] or the sequential model [2], or combinations of both. However, no matter the nature of the conformational change, and even without mechanistic information, it is possible to analyze the cooperative response by the use of phenomenological models.

In this paper, we focused our study in cooperative regulation of aquaporins (AQP) function. In particular, we will present results obtained for the plant AQP subfamily named PIP (for plasma membrane intrinsic proteins). Aquaporins are channels found in the three domains of life and most members of the family can transport water molecules across membranes. Structurally, all AQP are tetramers in which each protomer consists of a single aminoacidic chain with internal pseudo-twofold symmetry [3]. Aquaporin protomers folds in a way that six transmembrane helices, together with two half helices, are packed and form a hydrophilic pore for water (or other solutes) permeation. Thus, the quaternary conformation of each tetrameric AQP contains four pores, one in each protomer [4]. Despite most AQP are constitutively open channels, some members of this huge family are gated by pH [5–9]. In particular, plant PIP aquaporins have been well characterized as pH dependent channels [8,10–12].

Proton sensitivity has been characterized for PIPs belonging to different plant species such as *Arabidopsis thaliana* [8,13], red beet [10–12] and strawberry [14,15]. In all those cases a dose-response profile of biological activity *vs* proton concentration with sigmoidal shape was reported. PIP subfamily consist of two groups of paralogues (PIP1 and PIP2) that interact forming heterotetramers [16–19]. Those heterotetramers are also proton-sensitive and show a behavior well described by a sigmoidal function [11,12,14]. The sigmoidal shape of PIP proton dose-response curves suggests that water transport through these channels is a cooperatively regulated phenomenon. Structural studies revealed that open (related to the high-water transport activity) and closed (related to the low-water transport activity) stages of PIP present a complex rearrangement of loop D that depends on, at least, the protonation of a histidine residue which modifies the interactions between this loop and cytosolic domains [20,21] (Figure 1). Phosphorylation events and calcium levels are also reported as involved in PIP gating, but their participation is not yet fully elucidated [15,22,23]. Although there is no complete information on the parameters that govern the process of protons binding to the key histidine residue, nor it is certain that this residue is the main one involved in the gating process, all the structural studies suggest that there are two stages involved in the process: PIP protonation and conformational reorganization.

In previous works we investigated the ways in which PIP2 and PIP1 monomers from *Beta vulgaris* assemble in homo and heterotetramers, and how water transport is controlled by intracellular proton concentration [12,24]. In those works we showed that: i- the homotetramers of PIP1 are retained in the cellular interior while the homo-tetramers of PIP2 form functional tetramers that are located in the plasma membrane, ii- some PIP1-PIP2 pairs form heterotetramers of variable stoichiometry that depends on the available amount of each mRNA, and iii- the response of biological activity of heterotetramers, at different concentrations of protons, presents a pH half-maximal inhibition ($pH_{0.5}$) shifted to more alkaline values in comparison with the obtained for PIP2 homotetramers, similar results have been reported for strawberry aquaporins [14].

Our goal now is to thoroughly investigate the cooperativity in PIP aquaporins to understand the profiles found for homo and heterotetramers and offer a precise mathematical description of the experimental results. Moreover, simulations of the resulting phenomenological models allow us to clarify the effect of mixed populations of PIP oligomers in cell membranes.

RESULTS

1- Two-stage models for PIP cooperativity

To study cooperativity in PIP aquaporins it must be considered that these channels can hetero-oligomerize, which means that several assemblies with different stoichiometry are possible within a single cell expressing a minimum of two paralogues [25]. So, to investigate the cooperative response of PIP species in the heterologous expression system of Xenopus oocytes, we injected cRNA coding for PIP2 monomers, or for PIP2-PIP1 dimers, and performed water transport experiments. The injection of cRNA coding for PIP2 only allows the formation of PIP2 homotetramers, while the injection of cRNA coding for PIP2-PIP1 dimers only allows the formation of only PIP2-PIP1

heterotetramers with 2:2 stoichiometry. The strategy of creating a chimeric concatenated gene, encoding protein subunits connected by flexible linkers has been widely used to study unique molecular species of homo or hetero-oligomeric channels [12,26–28].

As outlined above, structural studies on PIP pH gating suggest that two stages are involved in PIP cooperativity, protonation of active tetramer (R) and conformational rearrangement.

$$\text{Stage I } R + nH^+ \leftrightarrow RH_n \qquad \text{(I)}$$

$$\text{Stage II } \mathrm{RH_n} \leftrightarrow \mathrm{RH_n^{low}} \qquad \text{(II)}$$

We proposed two different two-stage models accounting for PIP biological activity regulation to gain insight into the cooperativity of PIP2 homotetramers and PIP2-PIP1 (2:2) heterotetramers. One of these models considers that in PIP pH modulation (i.e. osmotic water permeability P_f vs. oocyte internal proton concentration) the cooperative step is the proton binding, and that the subsequent conformational modifications are independent for each protomer (MODEL 1); the other model assumes that the proton binding is a non-cooperative process and that the subsequent conformational rearrangement, or transduction event, is cooperative (MODEL 2).

Model 1: Cooperativity in proton binding

As mentioned before, this two-step model consists in a cooperative binding of protons followed by a non-cooperative conformational transduction event.

Step 1: Proton Binding

In this model the degree of protonation (α) will depend on the proton concentration [H^+] according to a Hill equation:

$$\alpha = \frac{[H^+]^{n_H}}{K^{n_H} + [H^+]^{n_H}} \qquad (1)$$

It must be stressed that the constant K and the Hill coefficient n_H do not represent the real equilibrium constant and the number of binding sites. In its place, K represents the proton concentration that produces half-maximal response ($[H^+]_{0.5}$), and n_H an empirical coefficient giving account of the mismatch respect to the hyperbolic behavior [29].

Step 2: Change in PIP water permeability or conformational transduction

This step represents the conformational rearrangement that occurs to transform the high permeability (RH_n), or open stage, into the low permeability (RH_n^{low}), or close stage, of the PIP tetramer (Scheme II).

In this model the water permeability, P_f, will depend linearly on the degree of protonation (α) as,

$$P_f = P_{fmax} - (P_{fmax} - P_{fmin}).\alpha \qquad (2)$$

Being $P_{f\ max}$ and $P_{f\ min}$ the maximum and minimum values in the dose-response curve. Replacing equation (1) in (2) and normalizing the water permeability (Γ) according to Equation 7 gives:

$$\Gamma = 1 - \frac{[H^+]^{n_H}}{K^{n_H} + [H^+]^{n_H}} \qquad (3)$$

Model 2: Cooperativity in conformational transduction

This two-step model consists first in a non-cooperative binding of protons followed by a cooperative conformational transduction to reach different permeabilities stages.

Step 1: Proton binding

In this model the degree of protonation (α_i) of identical and independent sites is described by the Adair equation [30]:

$$\alpha_i = \frac{[H^+]}{k_0 + [H^+]} \qquad (4)$$

Where [H^+] is the proton concentration and k_0 is the microscopic proton dissociation constant for the residues involved in pH gating. We consider a value of k_0 = 1μM (which is a typical value for exposed histidine side chains) assuming that the protonation of loopD' histidine is representative of the protonation event responsible for the change in PIP water permeability (Figure 1).

Step 2: Change in PIP water permeability or conformational transduction

Again, this step represents the conformational rearrangements involved in transforming the high permeability (RH_n), or open stage, into the low permeability (RH_n^{low}), or close stage, of the PIP tetramer (Schema II). In this model, the transduction step is described by a differential logistic function of α_i :

$$\frac{\partial P_f}{\partial \alpha_i} = \frac{c}{(P_{fmax} - P_{fmin})}\left(P_{fmax} - P_f\right)\left(P_f - P_{fmin}\right) = c\,(1-\Gamma)\Gamma \qquad (5)$$

Being P_f the water permeability, P_{fmax} and P_{fmin} the maximum and minimum values in the dose-response curve, c a phenomenological coefficient giving account of the steepest relative change in the aquaporin activity and Γ, the normalized P_f (see Equation 7). A similar equation has been proposed to explain the lipid modulation of the catalytic activity for some membrane transporters [31]. In terms of our model, this parameter represents the efficiency of the transduction step between the protons binding and the water transport events.

Integrating equation (5), and replacing α_i by equation (4), the normalized water permeability will be:

$$\Gamma = 1 - \frac{1}{1+e^{-c\left(\frac{[H^+]}{k_0+[H^+]}-\frac{[H^+]_{0,5}}{k_0+[H^+]_{0,5}}\right)}} \qquad (6)$$

Being, $[H^+]_{0,5}$, the proton concentration for which the differential change in water permeability ($\frac{\partial P_f}{\partial \alpha_i}$) is maximal.

Both models were fitted to experimental data obtained for both PIP2 homotetramers and PIP2-PIP1 (2:2) heterotetramers water transport responding to cytosolic acidification (Figure 2). The best fit parameters values are shown in Table 1.

Values of the coefficients n_H (Model I) and c (Model II) obtained for oocytes expressing the PIP2-PIP1 heterotetramers are not different from the values corresponding to the expression of PIP2 homotetramer (Table I). Fitting Model I results in a n_H of approximately 9 for both PIP tetramers, while fitting Model II results in a c value ranging around 40 to 70. Any of these coefficients present a physical interpretation beyond the estimation of the steepness of the sigmoidal curve; in the first case n_H estimates the cooperativity of proton binding, while in the second case, c constitutes an indicator of the conformational transition cooperativity. With regards to pH sensitivity, both models show that homo and heterotetramers present a quite different $[H^+]_{0.5}$. The estimated values are not different among models, being approximately 0.33 µM for homotetramers and 0.17 µM for heterotetramers. The 90 % confidence regions for the regression parameters did not overlap, indicating that the observed differences were statistically significant (Figure 3).

Clearly, the transition from the open to close state needs more protons for homotetramers than for heterotetramers but the cooperativity of this transition is not altered.

2- Apparent low cooperativity in PIP co-expression

To shed light on the cooperative macroscopic response of mixed PIP aquaporins populations in a membrane, we simulated a situation in which different proportions of PIP2 homotetramers and PIP2-PIP1 heterotetramers (with 2:2 stoichiometry) are expressed (Figure 4). For this simulation we considered that the normalized permeability of a mixture of species is the linear combination of the individual responses of all the molecular species, each one weighted by the mole fraction of this species in the mixture. The obtained results show that depending on the relative amount of each molecular species, the whole dose-response curve presents different degrees of positive cooperativity. Interestingly, this spectrum denotes that when two co-expressed single aquaporins, having the same degree of cooperativity (same n_H or c) but different sensitivity to ligand (different $[H^+]_{0.5}$), an apparent lower cooperativity is revealed. In the case of PIP2 homotetramers and PIP2-PIP1 heterotetramers, the spectrum of apparent cooperativity coefficients reaches a minimum value when both molecules are in equal quantities, $X_{HD} \approx 0.5$ (Figure 4B), showing that mixtures of these two molecular species with high cooperativity gives rise to a membrane profile of low cooperativity, due to their different sensitivity to protons.

Figure 5 shows the experimental results corresponding to the co-expression of PIP2-PIP1 heterodimer plus PIP2 monomers. In this situation there are three different kind of molecular species mixed in the membrane: PIP2 homotetramers, PIP2-PIP1 (with 2:2 stoichiometry) heterotetramers and PIP2-PIP1 (with 3:1 stoichiometry) heterotetramers. We achieved a full biophysical characterization of PIP2 homotetramers and PIP2-PIP1 2:2 heterotetramers biological activity since we know for both molecules: i- their intrinsic permeabilities (previously reported [12]), ii- the cooperativity coefficients (Table 1), and iii- their corresponding pH sensing parameter, i.e. $[H^+]_{0,5}$ (Table 1). Using the phenomenological models developed in this study and taking into account the contribution of each tetrameric species to the plasma membrane water permeability [12], we elucidated the biophysical parameters that characterize the PIP2-PIP1 (with 3:1 stoichiometry) heterotetramer. The value obtained for n_H is similar to the one found for the other PIP tetrameric species, and $[H^+]_{0,5}$ is equal to (0.177 ±0.016) µM, not different from the one corresponding to the PIP2-PIP1 heterotetramer with 2:2 stoichiometric (Table 2). Pseudoexperimental data were then generated considering parameters shown in Table 2 and Model I was fitted both to experimental and pseudoexperimental data. The best fitted parameter values show a low cooperativity coefficient (3.82 ± 1.09) (Figure 5). This low cooperativity is denoted as "apparent" because each molecular species involved in the response displays high cooperativity for proton sensing by its own.

DISCUSSION

In the present work we took advantage of phenomenological models to explore the cooperative dependence of biological function of PIP aquaporins with intracellular proton concentration.

We considered two time-separated stages to properly analyze the impact of acidification in water transport by PIP aquaporins: a proton binding event and an open-closed conformational transition. This approach has proven to be very successful to deal with complex biological phenomena [32]. Moreover, we studied the response of not only PIP homotetramers, but also of PIP heterotetramers, where two different paralogues, PIP2 and PIP1, are assembled [12]. Since the biological response curves (P_f vs. proton concentration) are sigmoidal, a cooperative phenomenon should be considered. To elucidate the cooperative nature of the modulation of both PIP2 homotetramers and PIP2-PIP1 2:2 heterotetramers we designed experiments where single molecular species were expressed in Xenopus oocytes. For PIP2 it was achieved by injecting cRNA coding for PIP2 in oocytes, but for PIP2-PIP1 2:2 heterotetramers we used a covalently linked tandem dimer of PIP2 and PIP1 monomers. Several reports showed that the use of tandem protein dimeric constructions allows the study of channels with a determined composition in the Xenopus oocyte expression system [33–35]. We have used this strategy in a previous work to unravel the stoichiometry of the different PIP tetrameric assemblies showing that the construct designed was adequate [12]. Each of the two proposed models attributes the cooperative character to only one of the two involved stages: Model 1 to the proton binding to specific sites, and Model 2 to the conformational rearrangement that occurs in the channel to close the pore and block water transport. Both models accurately describe the biological activity of the two molecular species assayed, PIP2 homotetramers and PIP2-PIP1 heterotetramers, indicating that cooperativity of water transport by PIP can be either arising from the proton binding step or from the conformational change. Moreover, the values of the phenomenological parameters n_H and c for both PIP species are not significantly different (Table 1).

Interestingly, our analysis also showed that the experimentally determined cooperativity can be masking real cooperative degrees if channels with quite different ligand sensitivity are present in the same membrane, as in the case analysed here for proton sensitivity. This approach allows us to gain insights on cooperative transport in aquaporins channels where relevant proton binding sites are still no clearly elucidated and mixed populations of tetramers are expected due to the ensemble characteristics of this multiprotein family.

It is worth to mention that the majority of experimental transport studies in channels that can form hetero-oligomers are performed by co-expressing pairs of molecules. In this way, the models used to give account of experimental dose-response curves only include information corresponding to the final state of the system under study, *i.e* a membrane with a mixed population of hetero-oligomers. Our simulations show that a careful analysis must be done when extracting conclusions about the biophysical characteristic of oligomers if mixed populations can be present due to variable stoichiometry of the ensembles. Moreover, even working with unique molecular species, hidden information about the cooperativity of each individual binding site can be overlooked. A similar situation occurs when cooperativity in macromolecules with multiple binding sites and different ligand affinities showing Hill coefficients values lower than the unity is computed as negative if sites are not individually analyzed [29]. The relevance of this distinction, on mixtures of hetero-oligomers in the case of molecules with variable stoichiometry, or for multiple binding sites in the case of unique molecular species, should not be underestimated.

Regarding the possibility of mixed populations of PIP heterotetramers in a same membrane, there are reports of simultaneous expression of both PIP1 and PIP2 in different tissues or cell types [36–38]. It was also suggested that PIP2 and PIP1 interaction may be a specific property of each PIP2-PIP1 pair [39]. As it was previously reported [12], $pH_{0,5}$ for *Beta vulgaris* PIP is different depending on whether the tetrameric molecular specie is an homo or an heterotetramer (Table 1). Among AQP, this behavior has also been reported for *Fragaria x annanassa* PIP [14]. Interestingly, numerous channels present modifications in dose-response parameters characterizing its biological activity when paralogues hetero-oligomerize. We can mention two examples among the several cases available in the literature: i- for AKT2/KAT2 channels it was shown that depending on the expression level of the two genes, different homo- and heterotetrameric channel populations are produced and exhibit different gating properties and sensitivity to channel regulators [40], and ii- for ASIC1a/2a it was reported that heteromers co-exist with either ASIC1a or ASIC2a homomers within a same cell, all having distinct electrophysiological characteristics [41]. In the case of PIP2 homotetramers and PIP2-PIP1 heterotetramers, their different biological activity under the variation of the regulatory ligand - the intracellular concentration of protons- imposed a particular apparent response in the whole plasma membrane water transport capacity. While each molecular species has a strong cooperative response (high n_H or c coefficients, depending on the model selected), the presence of different molecular species in a same membrane displays a spectrum of apparent low cooperativity due to their $pH_{0,5}$. In the case of mixing two molecular species, a minimum value can be found when both are in equal quantities (Figure 4B). For PIPs, the ratio between mRNA (or protein) amounts of each group can vary considerably between different cell types, and despite heterotetramers have not been confirmed *in planta*, this data suggests that different PIP1 and PIP2 homo- or heterotetramers can co-exist. In fact, the possibility of random mixing between different PIP paralogues as subunits in tetramers

whose final stoichiometry only depends on the expression level of each paralogue, would allow a wide spectrum of cooperative responses with enhanced pH sensing range enriching the effective response of a cell membrane with a minimum of expressed molecules. In this way, the plant cell would have a fine mechanism of adjustment of the plasma membrane osmotic water permeability given by the regulation of PIP1/PIP2 expression levels under each physiological condition [17].

Finally, we would like to stress that phenomenological modeling has a central epistemic value which is not in opposition with the need of finding mechanistic explanations. In cases such as the aquaporin water transport dependency on proton concentration, there is no certainty on the number of relevant binding sites for protons. Despite it is possible to proposed mechanistic explanations showing that the protonation of only a few specific residues promotes the open to close transition, this kind of mechanistic model is clearly incomplete due to the promiscuous nature of protons as ligands for a huge number of potential binding sites. Besides, relations between binding of protons and conformational transitions can be too complex to be reduced to simple mechanisms. Of course, a combined experimental and molecular dynamic approach can shed light on the possible mechanistic events involved in the proton gating of PIP channels. In this scenario, the phenomenological models proposed in this work will constitute a consistent framework for building molecular models for PIP channels pH sensing. In regards of this proposed methodological pluralism, a similar perspective was raised from the philosophy of science where complementary accounts integrating mechanistic and dynamical explanations have been highlighted as fruitful in different areas of biological and biophysical research [42,43].

In summary, in this work we showed that cooperativity in water transport can be attributed to the binding of protons, as was usually considered, but also to the conformational transition stage, or even in both moments of the gating process. We also proved that simulation of phenomenological models constitutes a powerful tool to explore the composition of mixed populations of hetero-oligomeric channels subjected to a dose-response experiment. We state that different explanatory strategies (phenomenological and mechanistic models) are complementary and mutually supporting in research on biological systems with vast complexity such as the case of proton binding to a channel. So, for these intricated cases, we support that a plural perspective in which every relevant aspect of the biological phenomena can be explicated according to its nature.

MATERIALS AND METHODS

DNA constructions and *In vitro* RNA synthesis

PIP aquaporins used in the work are BvPIP2;2 (accession number GQ227846.1) and BvPIP1;1 (accession number GQ227845.1) here named as PIP2 and PIP1 respectively, for the sake of simplicity. PIP2 cDNA sequence was cloned into BglII and SpeI sites of a pT7Ts derived vector containing T7 RNA polymerase promoter and carrying the 5' and 3' translated regions of the *Xenopus laevis* β globin gene. Artificial heterodimers containing PIP2 covalently linked to PIP1 were prepared as detailed in previous work [12]. PIP2-PIP1 heterodimer construct contains 19 amino acids linking the coding regions of both PIP. All constructs were confirmed by DNA sequencing (Macrogen Inc, USA) before use. The capped complementary RNA (cRNA) encoding PIP2 or PIP2-PIP1 heterodimer were synthesized *in vitro* using the *mMESSAGE mMACHINE T7 High Yield*

Capped RNA Transcription Kit (Ambion, Austin, Texas, USA) as described previously [24]. The synthesized products were suspended at a final concentration of 0.1 μg μL^{-1} in RNAse-free water and stored at -20 ºC until use. Agarose gel electrophoresis and GelRed (BioAmerica Biotech Inc., USA) staining were used to check the absence of unincorporated nucleotides in the cRNA after every *in vitro* cRNA synthesis. The cRNA was quantified by fluorescence using the Quant-iT RNA Assay Kit (Invitrogen, UK) or by a micro drop plate reader (Take3 Plate) in the micro plate spectrophotometer PowerWave using Gen 5 software (Bio-Tek). Before injecting, cRNA was diluted in RNAse-free water to inject a proper amount per oocyte. *Xenopus* oocytes were microinjected with single cRNA or a mixture of cRNA coding for different PIP and incubated for three days at 18 ºC prior to performing the experiments.

Oocyte water transport assays

The osmotic water permeability (P_f) of injected or non-injected oocytes with cRNA was determined by measuring the rate of oocyte swelling, as detailed in a previous work [11,44]. Briefly, the internal pH of oocytes was acidified by pre-incubating them for 20 min in solutions of different pH (50 mM Sodium Acetate, 20 mM MES for the 5.8-6.8 pH interval or HEPES for the 7.0-7.4 pH interval), supplemented with mannitol 1 M until the desired osmolality was achieved (~200 mOsmol kg^{-1} H_2O). All osmolalities were determined using a vapor pressure osmometer (5520C Wescor Inc. USA). The swelling response was induced by transferring the oocytes to a 5-fold dilution of the same solution with distilled water keeping constant the solution pH. The internal pH was then calculated as described previously [11]. Changes in oocyte volume were video-monitored by a WB-99 color video-camera (1.3 MP, Panacom, China) attached to a zoom stereo-microscope (Leica L2, Leica, Germany). Oocyte swelling was video-captured in still images (each 5 s for 60 s) using the AMCaP version 9.20 (http://noeld.com/programs.asp?cat¼video#AMCap) and then the images were analyzed by treating each oocyte image as a growing sphere whose volume could be inferred from its cross-sectional area (software *Image J* version 1.37, http://rsb.info.nih.gov.ij/). P_f was calculated according to pioneer works [45,46].

Homology model

The modeling of the 3-dimensional structure of BvPIP2:2 was performed using SWISS-MODEL workspace [47]. SoPIP2;1 (2B5F) and (4IA4) have been used as templates for the open and closed state respectively. Figure 1 was create using VMD http://www.ks.uiuc.edu/Research/vmd/[48].

Data analysis, Model fitting and Simulation

Data shown in the present study were normalized to include in the analysis different oocytes batches and/or RNA masses injected,

$$\Gamma = \frac{(P_f - P_{fmin})}{(P_{fmax} - P_{fmin})} \qquad (7)$$

where $P_{f\ max}$ and $P_{f\ min}$ are the asymptotic maximal and minimal values of the oocyte water permeability (P_f) vs pH. Pseudoexperimental data were generated assuming that the normalized permeability of a given mixture is a linear combination of the normalized permeabilities of all the

components. each weighted by the mole fraction of this component in the mixture. Equations were fitted to the experimental (or pseudoexperimental) data by the non-linear regression procedure implemented on Excel spreadsheets [49]. Best-fitted parameter values were expressed as the mean ± S.E.M. Joint confidence regions for the regression parameters were calculated as described by Levi et al.[50]. The contribution of each tetrameric form to the plasma membrane water permeability was estimated as previously reported [12]. Briefly, when the cRNA coding for the heterodimer is co-injected with the cRNA coding for PIP2, the proportion of each population of tetramers (Φi) containing *i* subunits of PIP2-PIP2 dimers can be predicted by means of a binomial distribution [51–54] assuming that PIP1 and PIP2 monomers associate as dimers in a first step and the tetramerization occurs by dimerization of dimmers, as previously shown for other channels [51,55], and that the dimerization step is given randomly allowing different stoichiometries to be assembled:

$$\Phi_i = \frac{n!}{i!(n-i)!}\theta^i(1-\theta)^{n-1} \qquad (8)$$

where $n = 2$, i is equal to the number of PIP2-PIP2 dimers within the tetramer and θ is the PIP2 molar fraction. Total plasma membrane permeability due to PIP expression (P_{fT}) can be expressed as:

$$P_{fT} = \Omega_{2:2} * \Phi i_{2:2} + \Omega_{3:1} * \Phi i_{3:1} + \Omega_{4:0} * \Phi i_{4:0} \qquad (9)$$

where Φi correspond to the proportion of each population of tetramers containing *i* PIP2-PIP2 dimers obtained from the binomial distribution (Eq. 8), P_{fT} is considered as (Total P_f measured - P_f of non-injected oocytes)/total ng of injected cRNA, Ω corresponds to P_f given by the expression of each tetrameric specie at the plasma membrane.

AUTHOR CONTRIBUTIONS

FLGF and KA designed the investigation, VV, CJ and ACF performed the experiments, FLGF developed the models, FLGF and VV fitted the models, FLGF, VV and AGF prepared figures, VV, LGF and KA analyzed data, VV, GS, FLGF and KA wrote the main manuscript text. All authors reviewed the manuscript.

ACKNOWLEDGMENTS

This work was supported by ANPCYT (PICT 2016- 4224 to FLGF and PICT 2017-0244 to KA) and UBA (UBACYT 2018 0178 to KA and 0306 to FLGF). We thank Dr. Elgoyhen and Dr. Calvo (INGEBI, UBA-CONICET) for generously providing oocytes and Lucio Aliperti Car for critical reading of the manuscript.

COMPETING INTERESTS

The authors declares no competing interests.

REFERENCES

1 Monod J, Wyman J & Changeux JP (1965) on the Nature of Allosteric Transitions: a Plausible Model. *J. Mol. Biol.* **12**, 88–118.

2 Koshland DE, Némethy G & Filmer D (1966) Comparison of experimental binding data and theoretical models in proteins containing subunits. *Biochemistry* **5**, 365–85.

3 Walz T, Hirai T, Murata K, Heymann JB, Mitsuoka K, Fujiyoshi Y, Smith BL, Agre P & Engel A (1997) The three-dimensional structure of aquaporin-1. *Nature* **387**, 624–7.

4 Shi LB & Verkman AS (1996) Selected cysteine point mutations confer mercurial sensitivity to the mercurial-insensitive water channel MIWC/AQP-4. *Biochemistry* **35**, 538–44.

5 Németh-Cahalan KL, Hall JE & Ne KL (2000) pH and calcium regulate the water permeability of aquaporin 0. *J. Biol. Chem.* **275**, 6777–82.

6 Kaptan S, Assentoft M, Schneider HP, Fenton RA, Deitmer JW, MacAulay N & De Groot BL (2015) H95 Is a pH-Dependent Gate in Aquaporin 4. *Structure* **23**, 2309–2318.

7 Zeuthen T & Klaerke DA a (1999) Transport of water and glycerol in aquaporin 3 is gated by H(+). *J. Biol. Chem.* **274**, 21631–6.

8 Tournaire-Roux C, Sutka M, Javot H, Gout E, Gerbeau P, Luu DTD-T, Bligny R & Maurel C (2003) Cytosolic pH regulates root water transport during anoxic stress through gating of aquaporins. *Nature* **425**, 393–7.

9 Frick A, Järvå M, Ekvall M, Uzdavinys P, Nyblom M & Törnroth-Horsefield S (2013) Mercury increases water permeability of a plant aquaporin through a non-cysteine-related mechanism. *Biochem. J.* **454**, 491–499.

10 Alleva K, Niemietz CM, Sutka M, Maurel C, Parisi M, Tyerman SD & Amodeo G (2006) Plasma membrane of Beta vulgaris storage root shows high water channel activity regulated by cytoplasmic pH and a dual range of calcium concentrations. *J. Exp. Bot.* **57**, 609–621.

11 Bellati J, Alleva K, Soto G, Vitali V, Jozefkowicz C & Amodeo G (2010) Intracellular pH sensing is altered by plasma membrane PIP aquaporin co-expression. *Plant Mol. Biol.* **74**, 105–118.

12 Jozefkowicz C, Sigaut L, Scochera F, Soto G, Ayub N, Pietrasanta LII, Amodeo G, González Flecha FL, Alleva K, González Flecha FL & Alleva K (2016) PIP Water Transport and Its pH Dependence Are Regulated by Tetramer Stoichiometry. *Biophys. J.* **110**, 1312–1321.

13 Verdoucq L, Grondin A & Maurel C (2008) Structure–function analysis of plant aquaporin AtPIP2; 1 gating by divalent cations and protons. *Biochem. J.* **415**, 409–416.

14 Yaneff A, Sigaut L, Marquez M, Alleva K, Pietrasanta LI & Amodeo G (2014) Heteromerization of PIP aquaporins affects their intrinsic permeability. *Proc. Natl. Acad. Sci.* **111**, 231–236.

15 Yaneff A, Sigaut L, Gómez N, Aliaga Fandiño C, Alleva K, Pietrasanta LI & Amodeo G (2016) Loop B serine of a plasma membrane aquaporin type PIP2 but not PIP1 plays a key role in pH sensing. *Biochim. Biophys. Acta - Biomembr.* **1858**, 2778–2787.

16 Zelazny E, Borst JW, Muylaert M, Batoko H, Hemminga M a & Chaumont F (2007) FRET

imaging in living maize cells reveals that plasma membrane aquaporins interact to regulate their subcellular localization. *Proc. Natl. Acad. Sci. U. S. A.* **104**, 12359–64.

17 Jozefkowicz C, Berny MC, Chaumont F & Alleva K (2017) Heteromerization of Plant Aquaporins. In *Plant Aquaporins, From Transport to Signalling* (Chaumont F & Tyerman S, eds), pp. 29–46. Springer.

18 Fetter K, Van Wilder V, Moshelion M & Chaumont F (2004) Interactions between plasma membrane aquaporins modulate their water channel activity. *Plant Cell* **16**, 215–228.

19 Berny MC, Gilis D, Rooman M & Chaumont F (2016) Single Mutations in the Transmembrane Domains of Maize Plasma Membrane Aquaporins Affect the Activity of Monomers within a Heterotetramer. *Mol. Plant* **9**, 986–1003.

20 Frick A, Järvå M & Törnroth-Horsefiel S (2013) Structural basis for pH gating of plant aquaporins. *FEBS Lett.* **587**, 989–993.

21 Törnroth-Horsefield S, Wang Y, Hedfalk K, Johanson U, Karlsson M, Tajkhorshid E, Neutze R & Kjellbom P (2006) Structural mechanism of plant aquaporin gating. *Nature* **439**, 688–94.

22 Fischer M & Kaldenhoff R (2008) On the pH regulation of plant aquaporins. *J. Biol. Chem.* **283**, 33889–92.

23 Nyblom M, Frick A, Wang Y, Ekvall M, Hallgren K, Hedfalk K, Neutze R, Tajkhorshid E & Törnroth-Horsefield S (2009) Structural and functional analysis of SoPIP2;1 mutants adds insight into plant aquaporin gating. *J. Mol. Biol.* **387**, 653–68.

24 Jozefkowicz C, Rosi P, Sigaut L, Soto G, Pietrasanta LI, Amodeo G & Alleva K (2013) Loop A Is Critical for the Functional Interaction of Two Beta vulgaris PIP Aquaporins. *PLoS One* **8**, e57993.

25 Jozefkowicz C, Scochera F & Alleva K (2016) Two aquaporins, multiple ways of assembly. *Channels* **10**, 438–439.

26 Yang Y, Yan Y & Sigworth FJ (1997) How Does the W434F Mutation Block Current in Shaker Potassium Channels ? *J. Gen. Physiol.* **109**, 779–789.

27 Tu L & Deutsch C (1999) Evidence for dimerization of dimers in K+ channel assembly. *Biophys. J.* **76**, 2004–2017.

28 Tytgat J & Hess P (1992) Evidence for cooperative interaccions in potassium channel gating. *Nature* **359**, 420–423.

29 Cattoni DI, Chara O, Kaufman SB & González Flecha FL (2015) Cooperativity in Binding Processes: New Insights from Phenomenological Modeling. *PLoS One* **10**, e0146043.

30 Adair G. (1925) The Hemoglobin System: VI. The Oxygen Dissosiation Curve Of Hemoglobin. *J. Biol. Chem.*, 529–545.

31 Dodes Traian MM, Cattoni DI, Levi V & González Flecha FL (2012) A two-stage model for lipid modulation of the activity of integral membrane proteins. *PLoS One* **7**, 6–13.

32 Gunawardena J (2014) Time-scale separation - Michaelis and Menten's old idea, still bearing fruit.

FEBS J. **281**, 473–488.

33 Bagriantsev SN, Clark KA & Minor DL (2012) Metabolic and thermal stimuli control K 2P 2.1 (TREK-1) through modular sensory and gating domains. *EMBO J.* **31**, 3297–3308.

34 Zhuo R-G, Peng P, Liu X-Y, Yan H-T, Xu J-P, Zheng J-Q, Wei X-L & Ma X-Y (2016) Intersubunit Concerted Cooperative and cis-Type Mechanisms Modulate Allosteric Gating in Two-Pore-Domain Potassium Channel TREK-2. *Front. Cell. Neurosci.* **10**, 1–11.

35 Wollberg J & Bähring R (2016) Intra- and Intersubunit Dynamic Binding in Kv4.2 Channel Closed-State Inactivation. *Biophys. J.* **110**, 157–175.

36 Alexandersson E, Fraysse L, Sjövall-Larsen S, Gustavsson S, Fellert M, Karlsson M, Johanson U & Kjellbom P (2005) Whole gene family expression and drought stress regulation of aquaporins. *Plant Mol. Biol.* **59**, 469–84.

37 Heinen RB, Bienert GP, Cohen D, Chevalier AS, Uehlein N, Hachez C, Kaldenhoff R, Le Thiec D & Chaumont F (2014) Expression and characterization of plasma membrane aquaporins in stomatal complexes of Zea mays. *Plant Mol. Biol.* **86**, 335–50.

38 Besse M, Knipfer T, Miller AJ, Verdeil J-L, Jahn TP & Fricke W (2011) Developmental pattern of aquaporin expression in barley (Hordeum vulgare L.) leaves. *J. Exp. Bot.* **62**, 4127–4142.

39 Yaneff A, Vitali V & Amodeo G (2015) PIP1 aquaporins : Intrinsic water channels or PIP2 aquaporin modulators ? *FEBS Lett.* **589**, 3508–3515.

40 Xicluna J, Lacombe B, Dreyer I, Alcon C, Jeanguenin L, Sentenac H, Thibaud JB & Chérel I (2007) Increased functional diversity of plant K+ channels by preferential heteromerization of the Shaker-like subunits AKT2 and KAT2. *J. Biol. Chem.* **282**, 486–494.

41 Bartoi T, Augustinowski K, Polleichtner G, Gründer S & Ulbrich MH (2014) Acid-sensing ion channel (ASIC) 1a/2a heteromers have a flexible 2:1/1:2 stoichiometry. *Proc. Natl. Acad. Sci. U. S. A.*, 2–7.

42 Bonnie M, Green S, Fagan M & Jaeger J (2015) Explanatory Integration Challenges in Evolutionary Systems Biology. *Biol. Theory* **10**, 18–35.

43 Walmsley J (2008) Explanation in dynamical cognitive science. *Minds Mach.* **18**, 331–348.

44 Alleva K, Marquez M, Villarreal N, Mut P, Bustamante C, Bellati J, Martínez G, Civello M & Amodeo G (2010) Cloning, functional characterization, and co-expression studies of a novel aquaporin (FaPIP2;1) of strawberry fruit. *J. Exp. Bot.* **61**, 3935–45.

45 Zhang RB & Verkman AS (1991) Water and urea permeability properties of Xenopus oocytes: expression of mRNA from toad urinary bladder. *Am. J. Physiol.* **260**, C26-34.

46 Agre P, Mathai JC, Smith BL & Preston GM (1999) Functional analyses of aquaporin water channel proteins. *Methods Enzymol.* **294**, 550–72.

47 Arnold K, Bordoli L, Kopp J & Schwede T (2006) The SWISS-MODEL workspace: a web-based environment for protein structure homology modelling. *Bioinformatics* **22**, 195–201.

48 Humphrey W, Dalke A & Schulten K (1996) VMD: Visual Molecular Dynamics. *J. Mol. Graph.*

14, 33–38.

49 Kemmer G & Keller S (2010) Nonlinear least-squares data fitting in Excel spreadsheets. *Nat. Protoc.* **5**, 267–281.

50 Levi V, Villamil Giraldo AM, Castello PR, Rossi JPFC & González Flecha FL (2008) Effects of phosphatidylethanolamine glycation on lipid-protein interactions and membrane protein thermal stability. *Biochem. J.* **416**, 145–152.

51 Naso A, Montisci R, Gambale F & Picco C (2006) Stoichiometry studies reveal functional properties of KDC1 in plant shaker potassium channels. *Biophys. J.* **91**, 3673–3683.

52 Naranjo D (1997) Assembly of Shaker K-Channels from a Random Mixture of Subunits Carrying Different Mutations. In *From Ion Channels to Cell-to-Cell Conversations* pp. 35–46. Springer US, Boston, MA.

53 Ding S, Ingleby L, Ahern C a. & Horn R (2005) Investigating the putative glycine hinge in Shaker potassium channel. *J. Gen. Physiol.* **126**, 213–226.

54 Németh-Cahalan KL, Clemens DM & Hall JE (2013) Regulation of AQP0 water permeability is enhanced by cooperativity. *J. Gen. Physiol.* **141**, 287–95.

55 Veerappan A, Cymer F, Klein N & Schneider D (2011) The tetrameric α-helical membrane protein GlpF unfolds via a dimeric folding intermediate. *Biochemistry* **50**, 10223–30.

56 Khandelia H, Jensen MØ & Mouritsen OG (2009) To gate or not to gate: using molecular dynamics simulations to morph gated plant aquaporins into constitutively open conformations. *J. Phys. Chem. B* **113**, 5239–44.

TABLES

Table 1. Best fit proton sensing parameter values.

Data are expressed as mean ± SEM.

Molecule / Model		**(Model 1)**		**(Model 2)**	
		n_H	$[H^+]_{0,5}$ (µM)	c	$[H^+]_{0,5}$ (µM)
PIP2 (4:0)	●●	8.8±4.6	0.33±0.02	48±23	0.33±0.02
PIP2-PIP1 (2:2)	●●	9.9±2.6	0.168±0.005	67±17	0.175±0.006

Table 2: Properties of the molecular species form after co-expression of PIP2 monomer and PIP2-PIP1 tandem dimer.

	PIP2 (4:0)	**PIP2-PIP1 (3:1)**	**PIP2-PIP1 (2:2)**
Φ_i	0.6889	0.2822	0.0289
Ω_i^{max} (cm s^{-1} ng^{-1})	0.00149	0.00300	0.00345
n_H	8.8	9.0	9.9
$[H^+]$ (µM)	0.330	0.177	0.168

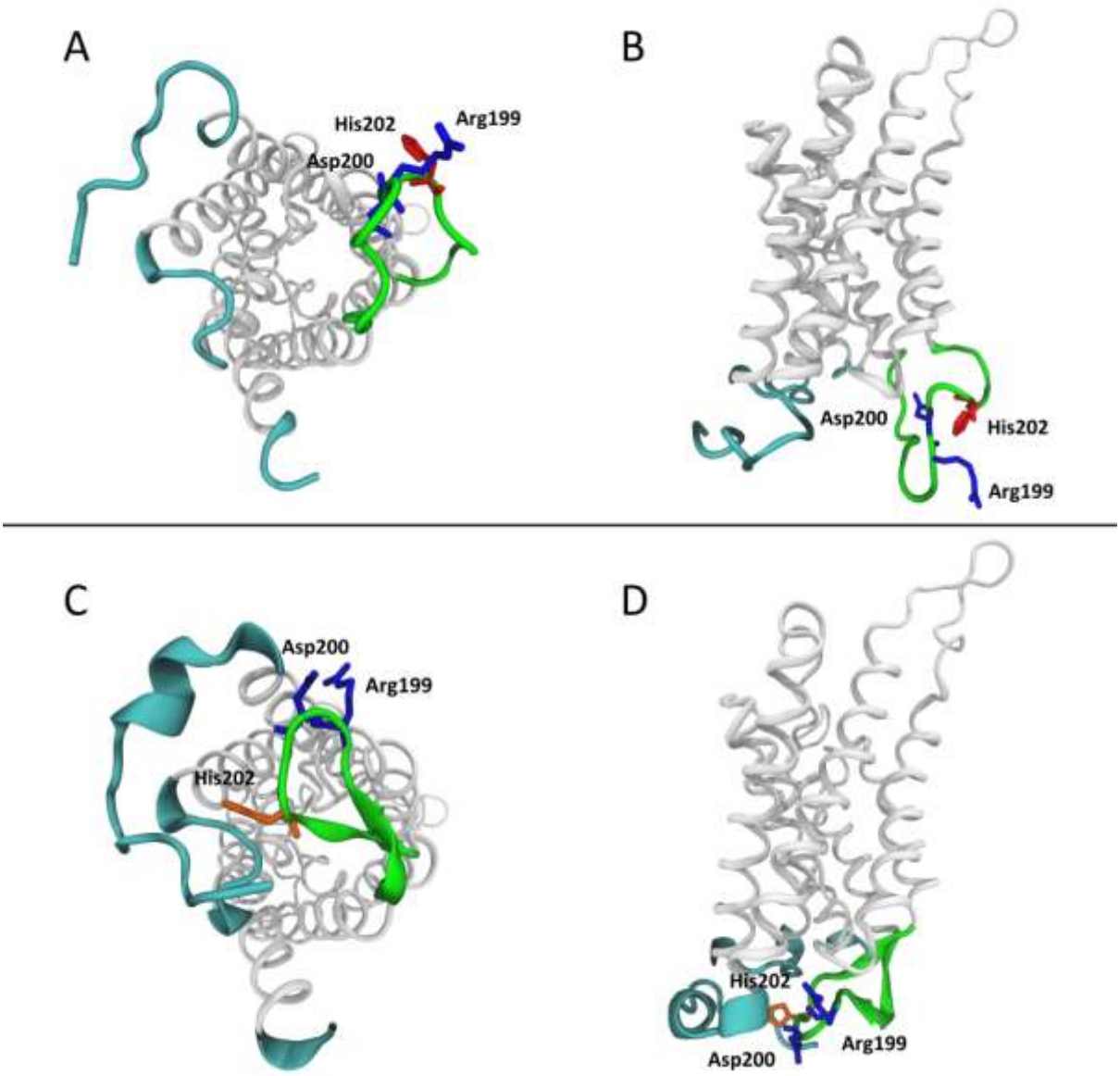

Figure 1. Structures of open (upper panel) and closed (lower panel) conformations of BvPIP2;2. Top (A/C) and side (B/D) views of BvPIP2;2 monomer shows that in an open stage (upper panel) loop D (showed in green) does not interact with other cytosolic domains (showed in cyan), while at closed stage (C, D) a conformational rearrangement occurs as consequence of interaction between cytosolic domains and the protonated residues, histidine (His202, protonated in orange; un-protonated in red), aspartic acid (Asp200, showed in blue) and arginine (Arg199, showed in blue) [8,56].

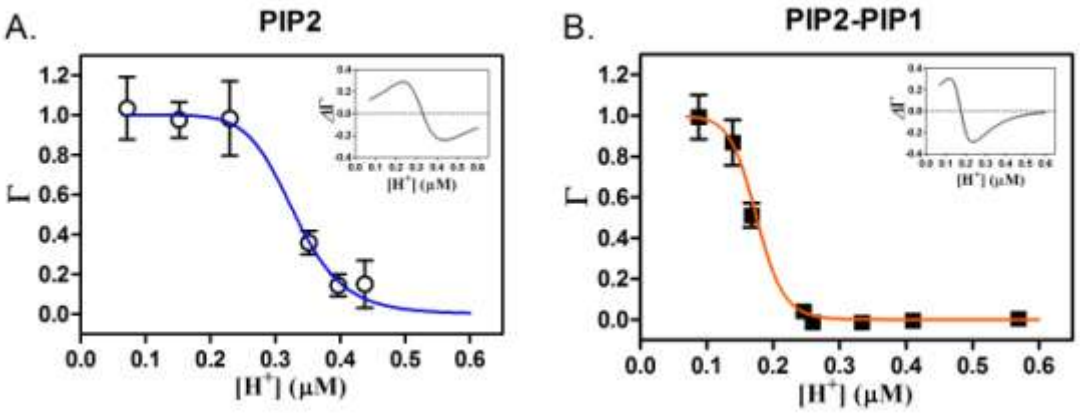

Figure 2. Dependence of the normalized water permeability (Γ) on the intracellular pH for oocytes expressing PIP2 homotetramers or PIP2-PIP1 heterotetramers. After cytosolic acidification P_f was tested in oocytes co-injected with equal amounts of cRNA coding for PIP2 (A) or PIP2-PIP1 tandem dimers (B). For each condition, values are shown as mean Γ± SEM, n= 8-12 oocytes tested in one representative experiment among 3 replicates with similar results. Continuous lines are the graphical representation of equation 3 and 6 fitted to the experimental data. Insets show the difference between the best fitting of Model I and Model II (ΔΓ).

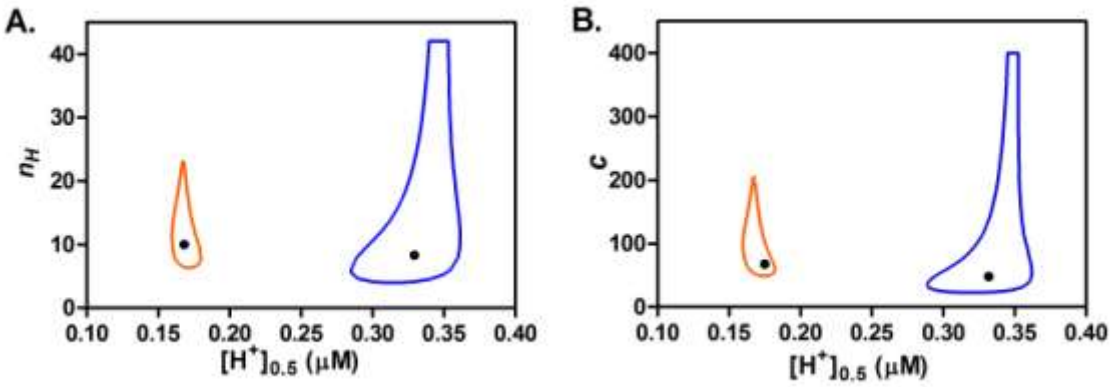

Figure 3. Confidence regions for cooperativity parameters. 90% confidence regions for the coefficients n_H;$[H^+]_{0.5}$ (A) and c;$[H^+]_{0.5}$ (B) were obtained after fitting equations 3 and 6 to experimental data of PIP2 or PIP2-PIP1 dimer shown in Fig. 2. Dots corresponds to the best fit parameter values shown in Table 1.

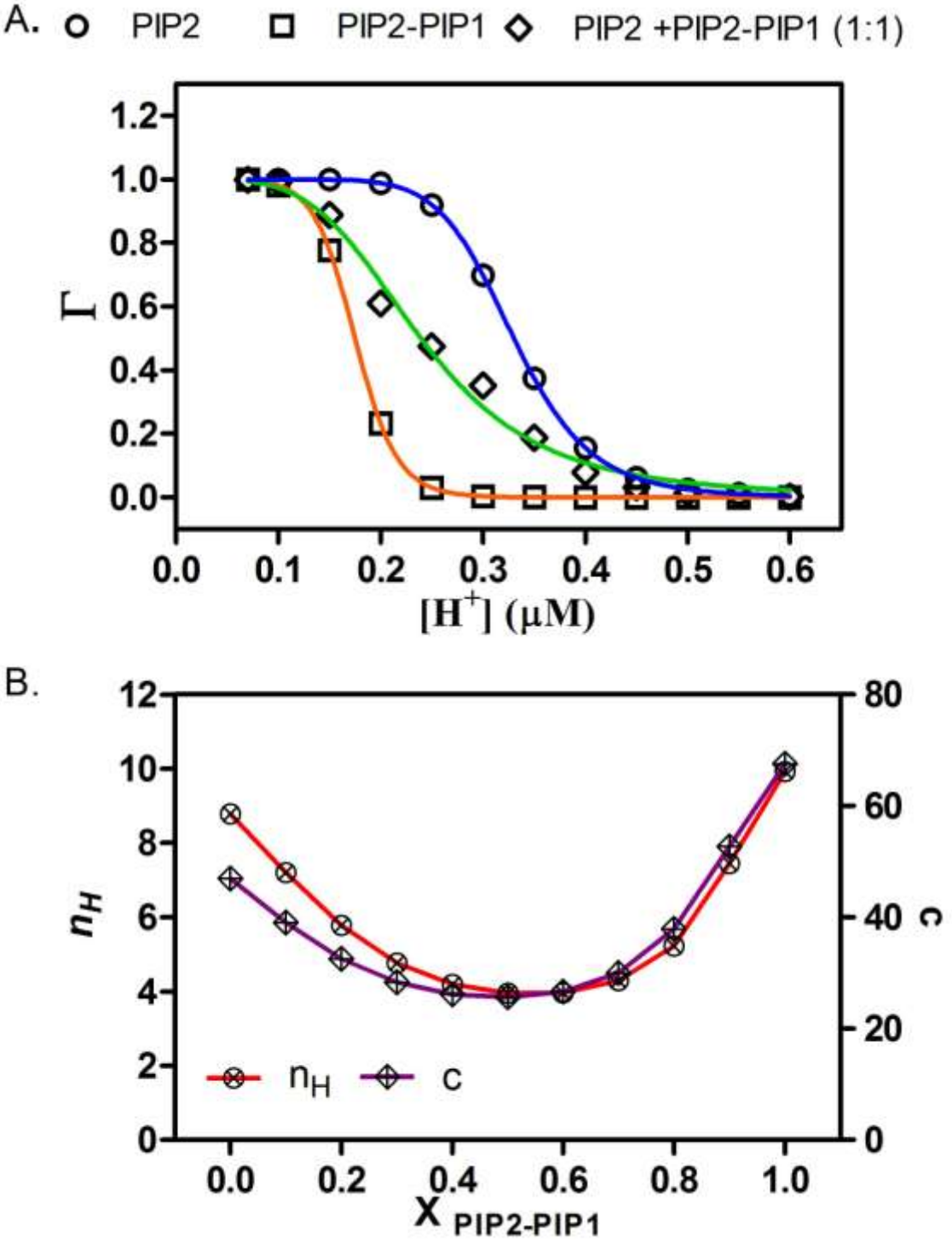

Figure 4. Changes in the apparent degree of cooperativity in PIP aquaporins mixtures. A: Pseudoexperimental data were simulated at 12 fixed $[H^+]$ values in the range 0.1-0.6 μM using equation 3 and 6 with the best fit parameter values shown in Table I for PIP2 homotetramers (○) and PIP2-PIP1 heterotetramers (□). An equimolar mixture of PIP2 homotetramers and PIP2-PIP1 heterotetramers (◊) was simulated calculating the normalized permeability at each $[H^+]$ as:

$\Gamma = \Gamma_{PIP2}$. XPIP2 + $\Gamma_{PIP2\text{-}PIP1}$. XPIP2-PIP1 with XPIP2 = XPIP2-PIP1 = 0.5. Continuous lines are the graphical representation of equations 3 and 6 fitted to the pseudoexperimental data. B: The same procedure was repeated for different mole fractions of homo and heterotetramers considering that in all the cases XPIP2 + XPIP2-PIP1 = 1. The best fit values of parameter n_H and c are represented as a function of the mole fraction of heterotetramer in the mixture.

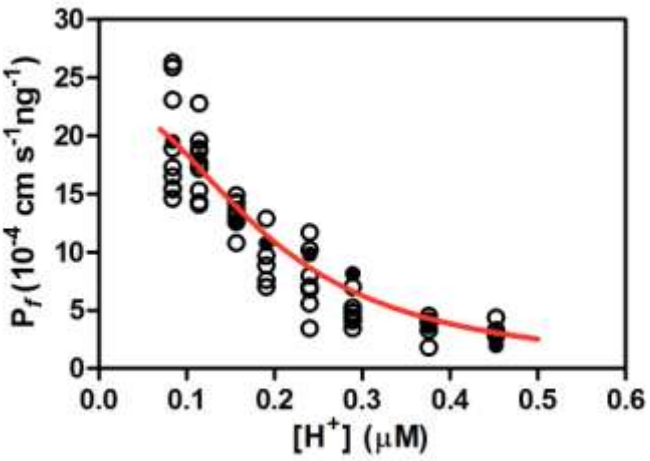

Figure 5. Dependence of water permeability (P_f) on the intracellular pH for oocytes expressing PIP2 homotetramers and PIP2-PIP1 heterotetramers. After cytosolic acidification P_f was tested in oocytes co-injected with 2.5 ng of PIP2-PIP1 tandem dimers cRNA and 5 ng of PIP2 cRNA. Open circles represent experimental data of one representative experiment among 3 replicates with similar results, black circles represent pseudoexperimental data generated with the values shown in Table 2, and continuous red line is the graphical representation of equation 3 fitted to the pseudoexperimental data.